Controlling factors of GaN wear

Guosong Zeng

Guosong Zeng[1], Xiaofang Yang[2], Charles H. Skinner[3], Bruce E. Koel[2], Nelson Tansu[4], Brandon A. Krick[1]
[1] Department of Mechanical Engineering and Mechanics, Lehigh University, PA, USA
[2] Department of Chemical and Biological Engineering, Princeton University, NJ, USA
[3] Princeton Plasma Physics Laboratory, NJ, USA
[4] Center for Photonics and Nanoelectronics, Department of Electrical and Computer Engineering, Lehigh University, PA, USA

Editor's Note: This month TLT profiles the 2016 recipient of **The E. Elmer Klaus Fellowship**, Guosong Zeng (Lehigh University). The Klaus Fellowship, along with The E. Richard Booser Scholarship, are awarded annually to graduate and undergraduate students, respectively, who have an interest in pursuing a career in tribology. As a requirement for receiving an STLE scholarship, students are given the opportunity to participate in a tribology research project and to submit a report summarizing their research.

Guosong Zeng received his bachelor's of science in measurement and control technology and instrumentation from Tianjin University in Tianjin, China, in 2010. He received his master's of science in mechanical engineering from Lehigh University in Bethlehem, Pa., in 2012. Since 2013 he has been pursuing his doctorate in mechanical engineering at Lehigh University. His research interest includes materials tribology, III-Nitrides, SiC and other coatings and surface physics and chemistry. You can reach him at **guz210@lehigh.edu**.

ABSTRACT

The optoelectronic properties of gallium nitride (GaN) have been well studied for decades, with results being translated to applications in solid state lighting and lasers, thermoelectricity, solar cells, power electronics, etc. However, the mechanical and tribological properties of GaN have been studied and understood far less than its optoelectronic properties. Our research aims to explore the wear performance of GaN and the controlling factors that will affect its wear rate. Directionality of GaN wear rate was observed with 60° periodicity. The local highest wear rate appeared along $<1\bar{2}10>$ *while the local lowest wear rate appeared along* $<1\bar{1}00>$*. The experimental results revealed that, the wear rate of GaN increased over 30 times when the testing environment changed from low humidity air to high humidity lab air. AES and SEM/EDS were employed to analyze the surface chemistry inside and outside the wear scar. The results provided further insight into the tribochemistry of GaN wear against alumina under different humidity environments.*

INTRODUCTION

The prevalence of gallium nitride (GaN) in scientific research and industrial engineering applications has rapidly expanded in recent years because of its outstanding electronic and optoelectronic properties [1–5], including its wide band gap. The progress in the GaN-based semiconductors were driven primarily on the material epitaxy and device innovations, enabling the wide implementation in power electronics [1] and solid state lighting technologies [2–5]. The progress in material innovation, specifically improvements of the dislocation density in GaN [6–11] and p-type doping activation [12–14], were the primary incentive and driving force of the III-Nitride technologies in the early period. More recent progress (the last decade) has been made through understanding of the nanostructure-property-performance physics and device, resulting in high efficiency nitride-based solid state lighting technologies [15–20]. The large bandgap in GaN-based semiconductors also makes these materials suitable for power electronics applications [1]. The importance of GaN-based innovation was recently recognized by the 2014 Nobel Prize in Physics [21].

In the pursuit of the advances in solid state lighting, lasers, and power electronics, tremendous advances were achieved on the understanding of the

electronics and optoelectronics properties of GaN-based materials, devices, and nanostructures. However, the mechanical properties and performance of GaN have far fewer studies. The lack of the investigation of the mechanical properties of GaN results in relatively few applications in mechanical or combined area. Elastic constants of GaN have been determined mainly by static displacement method, X-ray diffraction, resonance ultrasound method and acoustic wave method [22–25], and these parameters have been widely used in lattice mismatch and piezoelectric polarization effect [26–28]. The Young's modulus (210-330 GPa) and hardness (12-20 GPa) of GaN have been obtained by nanoindentation and bending test on suspended GaN microstructure [29–33]. The fracture toughness and yield strength of bulk single crystal GaN were also obtained by indentation and were found to be 0.79 ± 0.1 MPa√m and 15 GPa, respectively [31, 32]. The mechanism of plastic deformation under nanoindentation was also studied by Kucheyev et al. [33], they found that there was no systematic dependence of mechanical properties of GaN epilayer on both the coating thickness and the doping type and that slip-planes are one of the physical mechanisms responsible for the plastic deformation of GaN. An in-situ micro-compression test has been conducted to extract the deformation parameters of MOVPE grown GaN micro-pillars. Deformation was observed only occurring through 2nd order pyramidal slip on the $\{11\bar{2}2\}$ $\langle 11\bar{2}3 \rangle$ slip system and measured activation energy for the slip system was determined to be 0.91 ± 0.2eV and the Peierl's stress was 3.76GPa [34].

Even less is known about the tribological (friction and wear) properties of GaN and other III-Nitride materials (*i.e.* doped GaN and InGaN). GaN plays a key role in modern semiconductor industry; thus, it is crucial to understand its wear behavior and reliability, especially in MEMS devices, or under some harsh working environments (like space, desert, etc). Moreover, the study of friction and wear of GaN will be very conducive for understanding the machinability of GaN when we refer to the fabrication (ultraprecision machining, wafer grinding, micro/nano milling, etc.) of GaN-based devices. With nanoscratching, Lin et. al. showed substrate orientation dominated the extent of ploughing in GaN epilayers and c-axis sapphire-grown GaN epilayer has higher shear resistance than those GaN epilayers grown on a-axis sapphire substrate [35]. However, nanoscratch experiments are generally limited in the context of tribological performance because they are limited to one sliding cycle of a very sharp tip at relatively large contact pressures.

We measured the wear rate of GaN using custom pin-on-disk tribometers. The worn surface was analyzed by several surface characterization techniques. The results indicate that GaN has ultralow wear rate when tested under low humidity environment while tribochemical reaction took place and dominated the wear process when tested under high humidity environment. Rotary test revealed that wear performance of GaN has directionality with highest wear rate along $\langle 1\bar{2}10 \rangle$ and lowest wear rate along $\langle 1\bar{1}00 \rangle$.

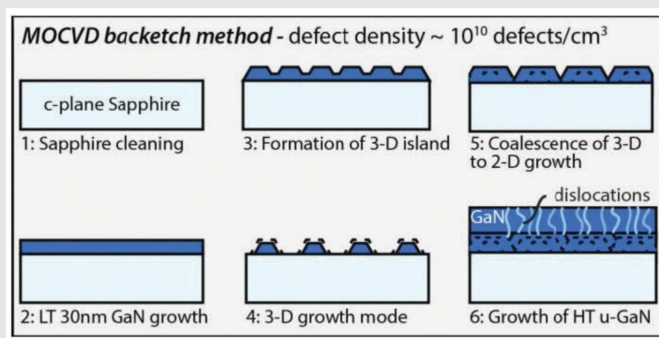

Figure 1 | **Illustration of MOCVD growth of GaN epilayer**

MATERIALS AND METHODS

Materials. 3µm thick single crystal undoped (0001)-GaN coating was grown by metal-organic chemical vapor deposition (MOCVD) on c-plane sapphire substrate. Ammonia and trimethylgallium were used as the precursors to obtain GaN, the chemical mechanism is shown Figure 1. The sapphire substrate was baked under 1080°C to remove all the contaminants and adsorbates. Then a 30-50nm thick GaN was grown on sapphire under low temperature, 530°C. To minimize the lattice mismatch induced strain at GaN/sapphire interface, the GaN lattice will rotate 30° with respect to Al_2O_3 unit cell, *i.e.*, $GaN_{[1\bar{1}00]}//Al_20_{3[1\bar{2}10]}$. When the growth of this low temperature GaN was done, the temperature was ramping up to 1090°C with ammonia overpressure inside the chamber to convert 2-D low temperature GaN into 3D GaN islands. A detector was used here to monitor the roughness of the coating. Once the surface roughness was low enough, the etching process would be stopped and the chamber would be backfilled with ammonia again together with trimethylgallium. GaN will first fill in the valley and the islands are gradually coalesced and eventually form a congruent, crystalline (Wurtzite) GaN coating.

Wear Test Methods. Both pin-on-disk rotary unidirectional dry sliding test and linear reciprocating dry sliding test were performed on the c-plane of Wurtzite GaN coating. The rotary testing was achieved by custom-built rotary stage (PI M-660.55) while the linear reciprocating sliding was achieved by a linear motor stage (Aerotech ANT95-L). The normal load was applied by using a double-leaf cantilever. Both normal force and frictional force were recorded for each cycle and the friction coefficient was calculated by averaging over the middle 20% of the stroke. 1.5mm diameter ruby (alumina) ball (Edmund Optics, Grade 25) was used as countersample due to its well-known chemical stability, hardness and wear resistance. The unidirectional rotary test was conducted at the velocity of 8mm/s with normal load of 400 mN in an ambient lab air environment with ~35±2%RH. The linear reciprocating sliding test was conducted at the velocity of 5mm/s with normal load of 600mN along $\langle 1\bar{2}10 \rangle$ crystal direction under both low humidity lab air (~10±2%RH) and high humidity lab air (~75±5%RH).

Wear Measurements. A scanning white light interferometer (Bruker ContourGT-I, optical profilometer) was employed here to map topography of the wear scars. For rotary test, a profilometric scan was made for every 3° and the corresponding wear rate was calculated. For linear reciprocating sliding test, 20 individual profilometric scans were made for each 5mm long wear scar and 5 cross-sectional line scans within each profilometric scan were extracted for wear rate calculation. These 100 cross-sectional line scans over 5mm long wear track were believed to minimize the uncertainties of the GaN wear rate due to local defect and contamination, non-uniform geometry, etc. The worn areas of these cross sections were evaluated by numerical integration and the averaged wear rate was obtained by applying Archard's wear rate, as shown in Eqn. 1.

$$K\left[\frac{mm^3}{N\cdot m}\right]=\frac{V[mm^3]}{F_n[N]\cdot d[m]}=\frac{A[mm^2]}{F_n[N]\cdot 2\cdot C}\cdot 10^3\left[\frac{mm}{m}\right] \quad (1)$$

A is the measured cross-sectional area of wear scar, C is for the number of reciprocating sliding cycles (one cycle includes one forward stroke and one reverse stroke), F_n is the applied normal load. A factor of 1000 [mm/m] here is used for unit consistency.

Coating Analysis. Scanning Auger electron microscopy, confocal Raman microscopy, atomic force microscopy (AFM) and scanning electron microscopy (SEM) were used here to characterize the worn and unworn surface.

AES is a state-of-the-art surface sensitive characterization technique and the typical probing depth is in the range of 10-50Å. In contrast to other surface characterization techniques, such as X-ray photoemission spectroscopy (XPS), surface extended X-ray absorption fine structure (SEXAFS), high resolution electron energy loss spectroscopy (HREELS), AES has better lateral and in-depth resolutions, which can perfectly fit into the wear scar. There is also no specific sample preparation requirement when compared to high resolution transmission electron microscopy (HR-TEM). Thus, AES was applied here to investigate the surface compositions of the wear scar. Confocal Raman spectroscopy (532nm laser band, lateral resolution 800nm) was also used here as a backup of AES analysis.

SEM (ZEISS 1550) was employed here to obtain the geometry of worn surface which was made under low humidity (~10±2%RH) and high humidity (~75±5%RH) environments. EDS (Oxford Instruments) was utilized here to compare distinguish the materials formed after the wear tests.

RESULTS AND DISCUSSIONS

Directionality

The rotary pin-on-disk experiment resulted in wear rates corresponding to all possible directions on the c-plane of GaN. The wear rate vs rotary track position (which correlates to crystallographic sliding direction) is plotted in Figure 2; this reveals that the wear rate of GaN exhibits a 60° periodicity, with local highest wear rate (peak) appears along <1$\bar{2}$10> and local lowest wear rate (valley) appears along <1$\bar{1}$00>. This is in consistence with our previous finding [36]. However, there still exists some factors that will locally change the wear performance of GaN. For instance, (1) the group III source (trimethylgallium) doesn't distribute evenly from center to edge of the substrate, which will lead to non-uniformity of surface geometry and (2) threading dislocation density varies from place to place. All these factors will result in fewfold of wear rate difference in same family direction.

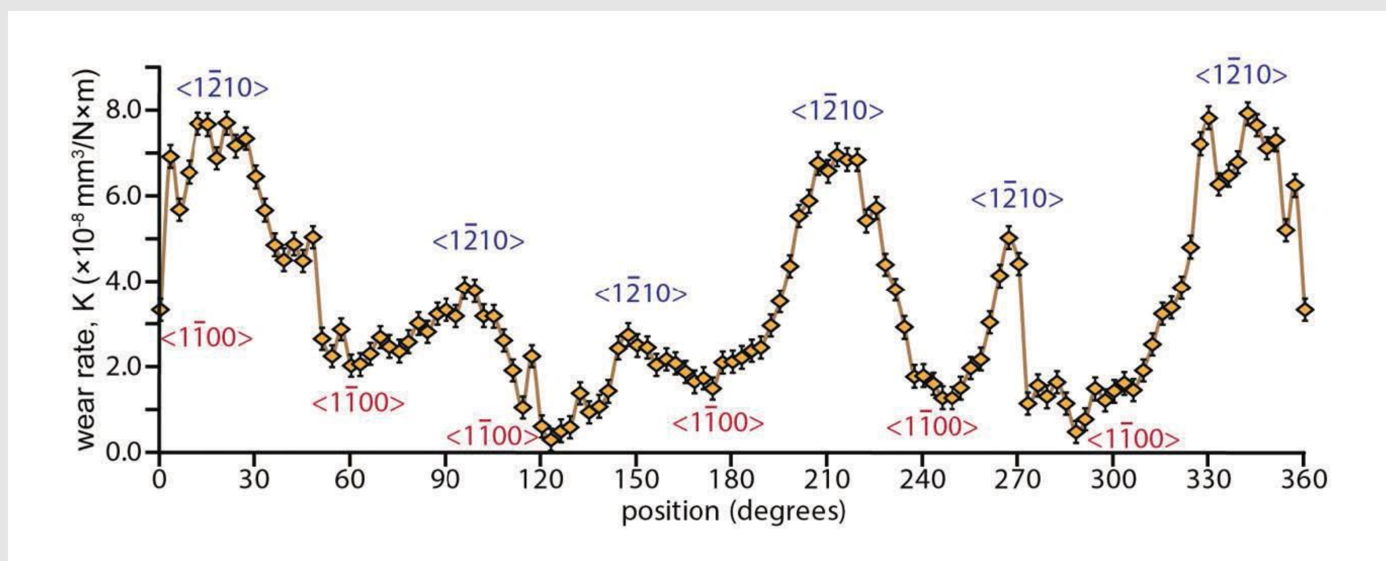

Figure 2 | **Directionality: GaN wear rate with respect to rotary stage position (and corresponding crystal direction): 400 mN normal load; 60,000 cycles; 1.5 mm diameter ruby probe; ~35% RH laboratory air**

Table 1 | **Wear rate of GaN under different environments**

environment		$K_{<1\bar{2}10>}$ ($\times 10^{-8}$ mm^3/Nm)	$\mu_{<1\bar{2}10>}$
Low humidity	**~10 % RH**	2.15 ± 0.70	0.2176 ± 0.0113
High humidity	**~75 % RH**	56.7 ± 1.94	0.2786 ± 0.0359

Tribochemistry

Crystal direction <$1\bar{2}10$> was selected to examine the humidity effect on GaN wear behavior under low (~10%RH) and high (~75%RH) humidity ambient air environments. The wear rates (K) and friction coefficient (μ) for these three testing environments are listed in Table.1.

The wear rate of GaN varied was ~30 times greater in high humidity (K~ 57 mm^3/Nm in ~75% RH) as compared to low humidity (K~ 2 mm^3/Nm in <10% RH). This dramatic influence of moisture on the wear performance of GaN suggests possible tribochemistry.

AES was employed to analyze the worn surface obtained under high humidity environment. Figure 3a shows the SEM image of the interested region inside wear scar. Both mapping (Figure 3b) and line scan (Figure 3c) were performed to reveal the surface composition inside and outside the wear scar. The wear debris consists of gallium oxide. The gallium signal is slightly less inside the wear scar than the unworn surface. The intensity of nitrogen inside the wear scar is also deficient as compared to the unworn surface. The increased oxygen signal with minimal decrease in Ga signal suggests there is a thin oxide layer (possibly Ga_2O_3) on the surface. Furthermore, the lowest intensities for both Ga and N and highest intensity for O inside the wear scar appear in the

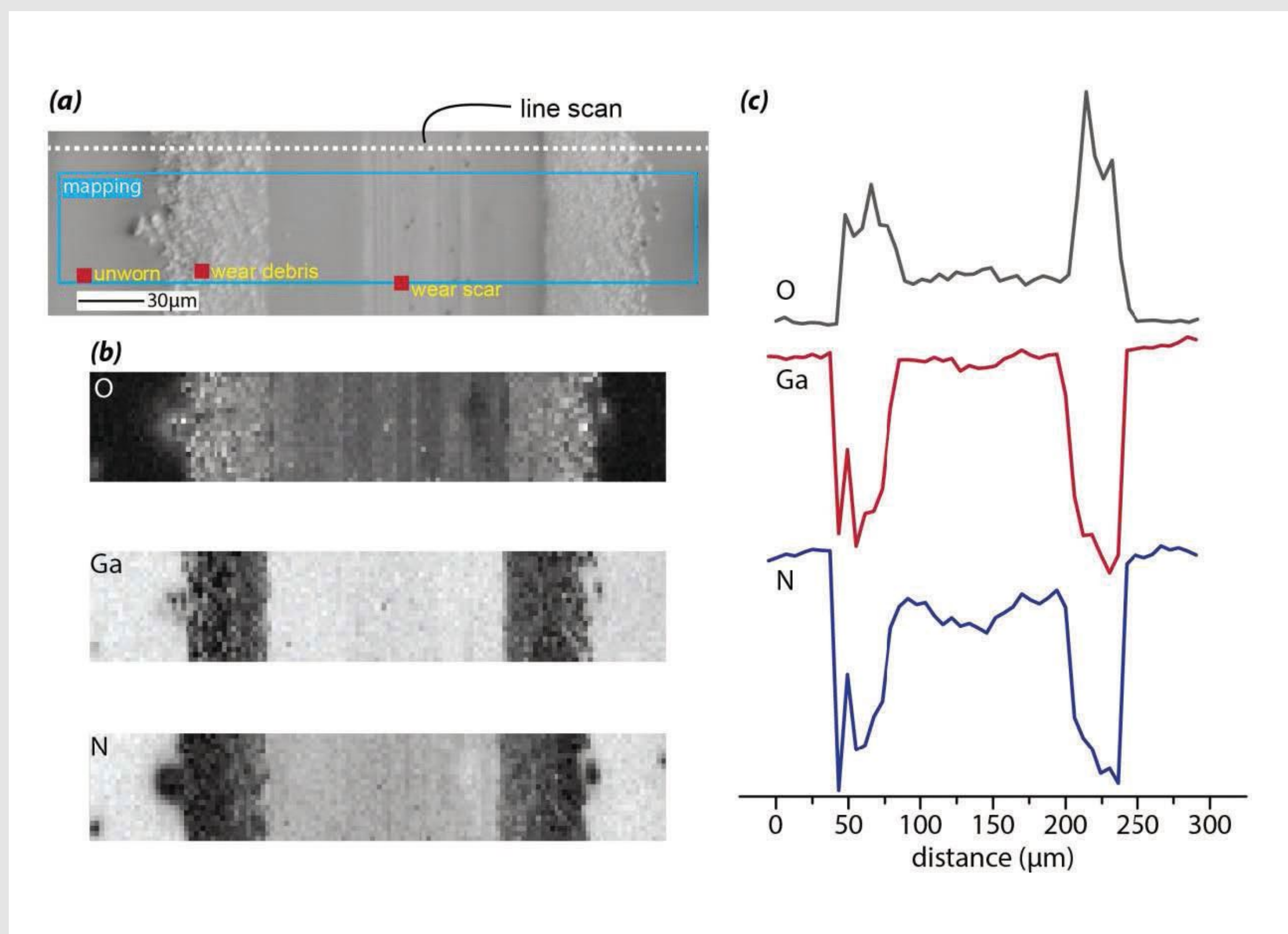

Figure 3 | **Auger electron spectroscopy, (a) SEM image of interested region, (b) Auger mapping and (c) line scan across the wear scar**

 Lightning is a discharge of electricity in the atmosphere. Lightning bolts can travel around 210,000 kph (130,487 mph) and reach nearly 30,000 C (54,032 F).

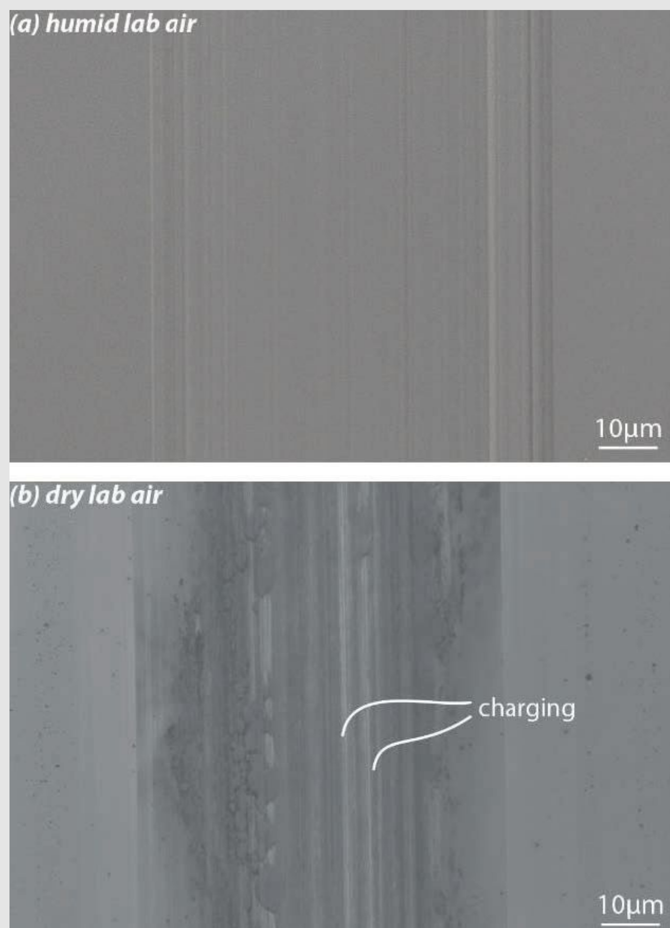

Figure 4 | **SEM images of high humidity and low humidity testing environments**

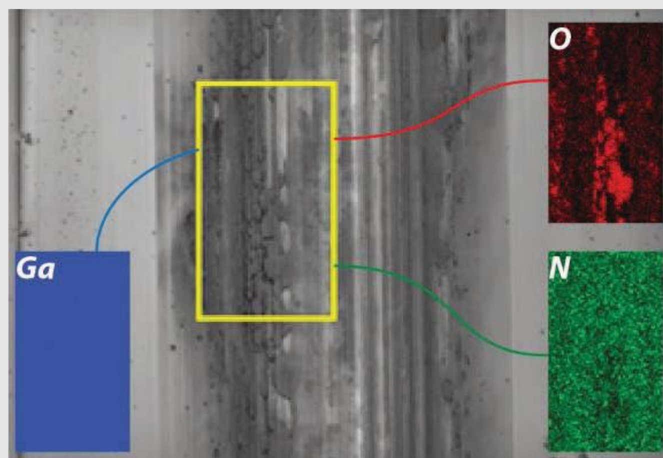

Figure 5 | **EDS Mapping of wear scar in low humidity environment**

center of the wear scar. This matches with the location of the maximum normal and shear stress.

Although GaN is believed to be chemical stable material [37, 38], oxidation of GaN can still happen with applied stress. Watkins et al. reported that GaAs has thicker oxide layer in stark contrast to GaN due to its larger lattice mismatch between GaAs and Ga_2O_3; this lattice mismatch will induce strain at the interface and lead to further oxidation of the subsurface material [38]. Similarly, we hypothesize the applied normal load and frictional load will open the GaN lattice and the stress will weaken the Ga-N bond, which makes water molecules easier to attack this material.

Confocal Raman microscopy shows no difference between worn and unworn surfaces (not shown here). The probing depth of Raman spectroscopy is about 1μm, which is much deeper than AES; this indicates that the oxide layer must be thin and exists only at the topmost surface.

SEM and EDS were also employed here to characterize the worn surfaces under different testing environments. Figure 4a and b show the SEM images of worn surfaces obtained by low humidity and high humidity lab air, respectively. We can see that the worn surface for low humidity air was covered by dark patches and had little charging. On the other hand, worn surface for high humidity air environment was smoother. EDS was revealed that the dark patches were mainly gallium oxide with rich oxygen signal and deficient signal of nitrogen inside the patches while gallium signal remained unchanged (Figure 5). Charging observed in low humidity testing environment wear scar also indicated the oxide layer formed on the worn surface.

To the contrast, EDS performed on the wear scar obtained under high humidity testing environment showed no signal of oxygen. The AES, Raman, SEM and EDS, collectively suggest that the oxide layer formed under high humidity environment was very thin and existing only at the topmost surface, which couldn't be detected by EDS and Raman, while AES was capable of probing first 10-50Å thick layer so that the oxygen signal can be measured.

CONCLUSION

Both directionality and moisture effect on GaN wear performance have been investigated. Rotary test showed the wear rate of GaN has a periodicity of 60° with highest wear rate along <$1\bar{2}10$> and lowest wear rate along <$1\bar{1}00$>. The increasing of wear rate from low humidity to high humidity environments was about 30 times. AES demonstrated the formation of thin gallium oxide during the wear test under high humidity environment. Stress was believed to assist the chemical reaction for forming this oxide layer. On the contrary, SEM and EDS revealed that thick oxide layer formed under low humidity testing environment.

ACKNOWLEDGEMENT

The authors would like to thank the Society of Tribologists and Lubrication Engineers for providing this E. Elmer Klaus Fellowship to support this research. The authors would also appreciate Dr. Chee-Keong Tan, Wei Sun, Damir Borovac for their valuable suggestions. TLT

REFERENCES

1. Mishra, U.K., Shen, L., Kazior, T.E., Wu, Y.F.: Gan-based RF power devices and amplifiers. *Proc. IEEE*. **96**, 287–305 (2008).
2. Pust, P., Schmidt, P.J., Schnick, W.: A revolution in lighting. *Nat. Mater.* **14**, 454–458 (2015).
3. Crawford, M.H.: LEDs for solid-state lighting: performance challenges and recent advances. *IEEE J. Sel. Top. Quantum Electron*. **15**, 1028–1040 (2009).
4. Tansu, N., Zhao, H.P., Liu, G.Y., Li, X.H., Zhang, J., Tong, H., Ee, Y.K.: III-nitride photonics. *IEEE Photonics J.* **2**, 241–248 (2010).
5. Tsao, J.Y., Crawford, M.H., Coltrin, M.E., Fischer, A.J., Koleske, D.D., Subramania, G.S., Wang, G.T., Wierer, J.J., Karlicek Jr., R.F: Toward smart and ultra-efficient solid-state lighting. *Adv. Opt. Mater*. **2**, 809–836 (2014).
6. Amano, H., Sawaki, N., Akasaki, I., Toyoda, Y.: Metalorganic vapor phase epitaxial growth of a high quality GaN film using an AlN buffer layer. *Appl. Phys. Lett*. **48**, 353–355 (1986).
7. Nakamura, S.: GaN growth using GaN buffer layer. Jpn. *J. Appl. Phys*. **30**, L1705–L1707 (1991).
8. Akasaki, I., Amano, H., Itoh, K., Koide, N., Manabe, K.: GaN-based ultraviolet/blue light emitting devices. *Inst. Phys. Conf. Ser.* **129**, 851–856 (1992).
9. Nakamura, S., Senoh, M., Mukai, T.: P-GaN/n-InGaN/n-GaN double-heterostructure blue-light-emitting diodes. Jpn. *J. Appl. Phys*. **32**, L8–L11 (1993).
10. Nam, O.H., Dremser, M.D., Zheleva, T.S., Davis, R.F: Lateral epitaxy of low defect density GaN layers via organometallic vapor phase epitaxy. Appl. *Phys. Lett*. **71**, 2638–2640 (1997).
11. Nakamura, S., Senoh, M., Nagahama, S., Iwasa, N., Yamada, T., Matsushita, T., Sugimoto, Y., Kiyoku, H.: Room-temperature continuous-wave operation of InGaN multi-quantum-well structure laser diodes. *Appl. Phys. Lett*. **69**, 4056–4058 (1996).
12. Akasaki, I., Amano, H., Kito, M., Hiramatsu, K.: Photoluminescence of Mg-doped p-type GaN and electroluminescence of GaN p-n junction LED. *J. Lumin*. **48–49**, 666–670 (1991).
13. Nakamura, S., Senoh, M., Mukai, T.: Highly p-typed Mg-doped GaN films grown with GaN buffer layers. Jpn. *J. Appl. Phys*. **30**, L1708–L1711 (1991).
14. Nakamura, S., Mukai, T., Senoh, M., Iwasa, N.: Thermal annealing effect on p-type Mg-doped GaN films. Jpn. *J. Appl. Phys*. **31**, L139–L142 (1992).
15. Feezell, D., Speck, J.S., DenBaars, S.P., Nakamura, S.: Semipolar (20-2-1) InGaN/GaN light-emitting diodes for high-efficiency solid-state lighting. *J. Disp. Tech*. **9**, 190–198 (2013).
16. Arif, R.A., Ee, Y.K., Tansu, N.: Polarization engineering via staggered InGaN quantum wells for radiative efficiency enhancement of light emitting diodes. *Appl. Phys. Lett*. **91**, 2005–2008 (2007).
17. Zhao, H., Liu, G., Zhang, J., Poplawsky, J.D., Dierolf, V., Tansu, N.: Approaches for high internal quantum efficiency green InGaN light-emitting diodes with large overlap quantum wells. *Opt. Express*. **19**, A991–A1007 (2011).
18. Yeh, T.W., Lin, Y.T., Stewart, L.S., Dapkus, P.D., Sarkissian, R., O'Brien, J.D., Ahn, B., Nutt, S.R.: InGaN/GaN multiple quantum wells grown on nonpolar facets of vertical GaN nanorod arrays. *Nano Lett*. **12**, 3257–3262 (2012).
19. Tan, C.K., Tansu, N.: Nanostructured lasers: electrons and holes get closer. *Nat. Nanotechnol.* **10**, 107–109 (2015).
20. Kim, H.J., Choi, S., Kim, S.S., Ryou, J.H., Yoder, P.D., Dupuis, R.D., Fischer, A.M., Sun, K.W., Ponce, F.A.: Improvement of quantum efficiency by employing active-layer-friendly lattice-matched InAlN electron blocking layer in green light-emitting diodes. *Appl. Phys. Lett*. **96**, 101102 (2010).
21. **http://www.nobelprize.org/nobel_prizes/physics/laureates/2014/.**
22. Savastenko, V.A., Sheleg, A.U.: Study of the elastic properties of gallium nitride. *Phys. Status Solidi*. **48**, K135–K139 (1978).
23. Polian, a, Grimsditch, M., Grzegory, I.: Elastic constants of gallium nitride. *J. Appl. Phys*. **79**, 3343–3344 (1996).
24. Schwarz, R.B., Khachaturyan, K., Weber, E.R.: Elastic moduli of gallium nitride. *Appl. Phys. Lett*. **70**, 1122 (1997).
25. Deger, C., Born, E., Angerer, H., Ambacher, O., Stutzmann, M., Hornsteiner, J., Riha, E., Fischerauer, G.: Sound velocity of Alx-Ga1-xN thin films obtained by surface acoustic-wave measurements. *Appl. Phys. Lett*. **72**, 2400–2402 (1998).
26. Ambacher, O., Majewski, J., Miskys, C., Link, A., Hermann, M., Eickhoff, M., Stutzmann, M., Bernardini, F., Fiorentini, V., Tilak, V., Schaff, B., Eastman, L.F: Pyroelectric properties of Al(In)GaN/GaN hetero- and quantum well structures. *J. Phys. Condens. Matter.* **14**, 3399–3434 (2002).
27. Bykhovski, A.D., Gelmont, B.L., Shur, M.S.: Elastic strain relaxation and piezoeffect in GaN-AlN, GaN-AlGaN and GaN-InGaN superlattices. *J. Appl. Phys*. **81**, 6332 (1997).
28. Christmas, U.M.E., Andreev, A.D., Faux, D.A.: Calculation of electric field and optical transitions in InGaN/GaN quantum wells. *J. Appl. Phys*. **98**, (2005).
29. Yang, Z., Wang, R.N., Jia, S., Wang, D., Zhang, B.S., Lau, K.M., Chen, K.J.: Mechanical characterization of suspended GaN microstructures fabricated by GaN-on-patterned-silicon technique. *Appl. Phys. Lett*. **88**, 1–3 (2006).
30. Tsai, C.H., Jian, S.R., Juang, J.Y.: Berkovich nanoindentation and deformation mechanisms in GaN thin films. *Appl. Surf. Sci*. **254**, 1997–2002 (2008).
31. Nowak, R., Pessa, M., Suganuma, M., Leszczynski, M., Grzegory, I., Porowski, S., Yoshida, F.: Elastic and plastic properties of GaN determined by nano-indentation of bulk crystal. *Appl. Phys. Lett.* **75**, 2070 (1999).
32. Drory, M.D., Ager, J.W., Suski, T., Grzegory, I., Porowski, S.: Hardness and fracture toughness of bulk single crystal gallium nitride. *Appl. Phys. Lett*. **69**, 4044 (1996).
33. Kucheyev, S.O., Bradby, J.E., Williams, J.S., Jagadish, C., Toth, M., Phillips, M.R., Swain, M. V.: Nanoindentation of epitaxial GaN films. *Appl. Phys. Lett*. **77**, 3373 (2000).
34. Wheeler, J.M., Niederberger, C., Tessarek, C., Christiansen, S., Michler, J.: Extraction of plasticity parameters of GaN with high temperature, in situ micro-compression. Int. *J. Plast*. **40**, 140–151 (2013).
35. Lin, M.H., Wen, H.C., Jeng, Y.R., Chou, C.P.: Nanoscratch characterization of GaN epilayers on c- and a-Axis sapphire substrates. *Nanoscale Res. Lett*. **5**, 1812–1816 (2010).
36. Zeng, G., Tan, C.K., Tansu, N., Krick, B.A.: Ultralow wear gallium nitride. *Appl. Phys. Lett*. **109**, 51602 (2016).
37. Prabhakaran, K., Andersson, T.G., Nozawa, K.: Nature of native oxide on GaN surface and its reaction with Al. *Appl. Phys. Lett*. **69**, 3212 (1996).
38. Watkins, N.J., Wicks, G.W., Gao, Y.: Oxidation study of GaN using x-ray photoemission spectroscopy. *Appl. Phys. Lett*. **75**, 2602–2604 (1999).

A bolt of lightning lasts less than a second and can measure up to three million volts.